Journal of Operation and Automation in Power Engineering

Vol. 12, No. 1, Jan. 2024, Pages: 77-90

http://joape.uma.ac.ir

Comparison of Transmission Line Models by Excluding Frequency Dependence in Complex Power System for Error Estimation

G.V.B. Chary *, *and K. Roslina*

Electrical and Electronics Engineering Department, VFSTR deemed to be University, Vadlamudi, Guntur, A.P, India

Abstract— *Today, commercial simulation packages can have the capability of solving complex power system networks by using various transmission line models. When there is a change in the modeling routine of transmission lines, their accuracy is also changese main aim of this paper is to compare lumped PI and distribute CP transmission line models in terms of accuracy and optimization capability. The IEEE 57 bus time domain power system models are designed by using these transmission line models for analysis in this paper. In these proposed systems the transmission line parameters are described as frequency independent. Therefore, in CP lines the Clark's transformation method does not provide exact decoupling of lines, to achieve exact decoupling of lines and accuracy the lines are continuously transposed in proposed systems. The NR load flow analysis was used for error estimation in balanced and unbalanced networks. The results had reported voltage error at the buses, transmission line error as function of line length and frequency response of line parameters. The frequency study of the line parameters was shown the PI lines system behaves as low pass filter and the CP lines system behaves as high pass filter. In this paper, also studied the optimization of proposed models by using a well-known Ant Lion Optimization (ALO) algorithm to set control variables, such as generator voltages, position of tap changing transformers and shunt capacitor banks. The optimization results of total power loss, voltage deviation and voltage stability index were compared with other algorithms. The results revealed that the ALO has best cothe nvergence characteristics and best elitism phase. Therefore, the CP lines system had shown considerable improvements of optimization results.*

Keywords—Clark's transformation, Complex power system, Constant frequency parameters, Distributed CP line, IEEE 57 test case, Lumped PI line, Modeling routine, NR load flow, Time-domain model.

1. INTRODUCTION

Transmission lines in the power system represent a major part among all other components. The accurate line models are very essential to the power system for accurate real time and parallel simulations. Otherwise, either underestimation of the voltage causes low rating of the tested equipment or overestimation of the voltage causes high rating of the tested equipment that would be effect on the cost of transmission lines. In single-phase and three-phase lines the skin effect in ground return wire leads to line parameters were frequencies dependent. Therefore, the closed mathematical solution of the line parameters in time domain is very difficult. The accuracy and efficiency of transmission lines for the transient period has discussed in [1–3].

In the power system the modeling the linear lumped π, T, and L transmission line models are obviously approximations only. While using these lines the error was can minimized by selecting sufficient number of per km sections, but it would increase the computational time of simulation. Because, generally the frequency error is proportional to the line length and the voltage error is inversely proportional to the number of sections [4]. Whereas the exact PI line model is more accurate than the nominal PI (i.e. product of line length and per km parameter) line model, it is preferably using in the place of long transmission lines [5].

Received: 17 Apr. 2022
Revised: 10 Jul. 2022
Accepted: 08 Aug. 2022
*Corresponding author:
E-mail: gvbc.eeep@gmail.com (G. V. B. Chary)
DOI: 10.22098/joape.2023.10656.1766
Research Paper

The propagation of voltage and current waves in the long multi conductor OH line was analyzing either in phase quantities or in model transformations methods [6, 7] in the time domain analysis. These two methods were generally considered the frequency dependence of transmission line parameters in the time domain solution [8–10]. Among various transformation matrix methods the Clark's transformation method was most widely known for analysis of transmission line over a wide range frequencies. When a 3-phase 400kV system was incorporated with single phase / double phase lines and they were in non-transposed line configuration, the lines were operated in three modes named as β (exact) and α-0(two quasi) modes. But if the same lines were using transposition configurations, they operated in α=β and 0 modes only. The references [11, 12] have shown the difference between the operations of both transmission line models under the transient conditions by considering the frequency dependence of line parameters. In the phase-mode-phase transformation the line was cannot decouple fully to LL and LG faults, but in the ABCD matrix method [13] the lines were completely decoupled. In the Clark's transformation method the two per two transformation matrix methods was used to accomplish exact decoupling of line, but this method was increasing 40% of simulation time. The effect of $[Z]$ and $[Y]$ matrixes with the ground-return wire was observed in 440kv transmission line [15]. Whereas in the implicit form these matrices were frequency dependent and they consist of mutual terms, but in explicit form the mutual terms were absent. By adding the soil conductivity (σ) and permittivity (ε), the effects of matrices were observed by using poorly conducting ground-return wire [16].

Normally, in the Bergeron's line model the transmission line parameters were represented as concentrated longitudinal (or) transversal. With the addition of the frequency effect in this model, by using vector fitting methods it was very useful to observe

the high frequency oscillations[17]-[18]. If the transmission line parameters were evaluating with the Universal Line Model (ULM) under transient conditions, such as switching, dynamic load, and faults. The differential equation solution of transmission line was using the ILT due to convolution integral. Whereas the PI line was directly developed by the numerical integration method, the time domain solutions of these models were consisted oscillations [19]. Based on the method of characteristics and recursive convolution, a new FD line model was developed [20], the performance of this model was verified by using the external field and compared in the EMTP. A multi-scale simulation based FD line model had developed for decoupling of transmission line modes and for diverse transients. It was observed that it can cover high frequency transients as shown in the EMTP and at low frequency transients with dynamic phasor of varying time-step size [21]. In the state-space method when the distribution lines were replaced by cascaded lumped sections lines, based on the number of PI sections in the line it can covers certain frequency range of analysis. The EMTP solution of these lines was can perform with the Eigenvector, Van-dermonde matrix, and Lagrange methods [22]. The solution of the modes decoupling in non-transposed lines as a function of the length was discussed by using the Exact, Conventional, and Mixed routines [23] line models, they have shown maximum 10% of peak error for the line length was varying from 10km to 1100 km.

When the transmission line modeling routine is changing, the losses in power system are also changing due to the variation of equivalent line parameters. These changes in power system can force the system operators to modify the optimization strategies to ensure for economic operation and satisfactory security constraints. The ORPD problem is very useful for assessment of power system planning and operation [24]. Moreover, it has considered as a complex optimization problem with non-linear characteristics. Over the decades various classical optimization methods have been used to solve this problem. Such as Newton Raphson (NR) method, Nonlinear programing (NLP) method, Quadratic programing (QP) method, and interior point method (IP) method. But due to lack of flexibility with real-time systems, more computation time when dealing with complex objective function, and dealing with control variables the complexity of ORPD problem was increased [25, 26]. Today, this problem is successfully solving by using various optimization algorithms, such as genetic algorithms (Gas), differential algorithm (DE), Simulated annealing (SA), Particle swarm optimization (PSO), Harmony search algorithm (HSA), Artificial bee colony algorithm (ABC), Gravitational search algorithm (GSA) etc. Generally most of the optimization problems were used calculated total generation cost of power system based on the total transmission loss as an objective function, but some power system researchers are using different objective functions either individually or in combination based on the application. This paper is used to describe minimization of total power loss with penalty functions, voltage deviation and voltage stability index by using meta-heuristic optimization techniques. This paper is using Ant Lion Optimizer (ALO) algorithm [27] to describe the variation control parameters of proposed transmission line models. It has follow the hunting nature of ant lion by using five main steps, such as random walk of ants, building traps, trapping of ants, catching preys and reconstruction of ant lion traps. This algorithm is mostly using for real world problems, it has high exploration capability of unknown search space, high convergence speed, and adaptive boundary shrinking mechanism property and elitism. This paper also considers another three algorithms to compare proposed power system models. Those are Grasshopper Optimization Technique (GOT) [28], Whale Optimization Technique (WOT) [29] and Spider Monkey Optimization (SMO) [30].

Accurate modeling of transmission lines for a time domain power system network is a complex task. The FD line models have limitations due to the non-linear wave propagation of voltage and current waves. But, on the other side, they have great accuracy

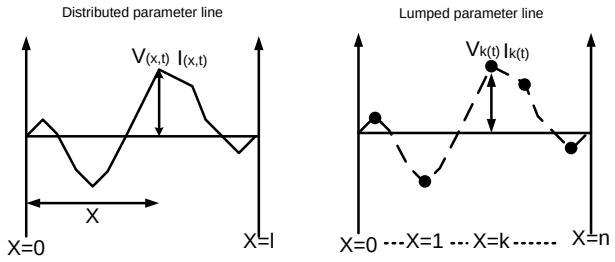

Fig. 1. Representation of the magnitude of voltage and current waves in transmission line models as a function of the line length

and provide wide range of frequency solutions. Normally, the solution of the differential equations of the lumped line models was affected by the error. To achieve accuracy they should be replaced with distributed parameters line models for time domain solution. The Clarke's transformation matrix solution is one of the methods using in the EMTP lines, in these lines when lines were un-transposed due to the asymmetric characteristics of $[Z]$ and $[Y]$ matrices, quasi modes would present in the solution. In this paper these modes were made zero by considering transposition of lines. This paper was reviewed and compared the accuracy of proposed systems when they are modeled by using lumped PI and continuously transposed CP lines. The present work is focused on the modeling and analysis of the 3–phase time domain models of IEEE 57 bus test case systems [24]. In power system models the line parameters are considered as frequency independent and calculated at 50Hz frequency. The performance of models was verified by using balanced and unbalanced load flow studies. In addition to these proposed models are optimized by using the minimization of total power losses, voltage deviation and voltage stability index. This was process described setting of control variables, such as generator voltages, transformer tap settings and shunt capacitors. The optimization of systems have verified with Ant Lion Optimizer (ALO) method, Also compared by using Grasshopper Optimization Technique (GOT), Whale Optimization Technique (WOT), and Spider Monkey Optimization Algorithm (SMO). The results show that the accuracy of CP lines when they are transposed, error as function of the transmission line length [23], and the frequency response of line parameters for high and low frequency of waves and optimization of systems.

This paper is organized as follows: Explained the mathematical formulation of lumped PI and distributed CP transmission line models at constant frequency, the real-time modeling of proposed power systems and overview of all power system components are discussed in Section 2. Objective function formulation, control variables and constraints are discussed in Section 3. Ant lion algorithm (ALO) and flow chart discussed in Section 4. Analysis of power flow results, transmission line errors, frequency response of line parameters, setting of control variables and convergence characteristics are discussed in Section 5. Followed by conclusion is in Section 6.

2. Transmission Line Models and Simulink Modeling

In this paper the proposed power system models are designed by using lumped PI and distributed parameters CP transmission line models. In the distributed line model the voltage ($V_{(x,t)}$) and current ($I_{(x,t)}$) waves are indexed as continuously propagated in line w.r.t space and time, but in the case of lumped line they are indexed as independent of time, therefore magnitude of waves described as series of points as shown in Fig. 1. The characteristics of these signals in the transmission line are depending up on the source frequency. If the source frequency is 50Hz, the lines should have to exceed 6000km before the propagation time significant. Whereas the frequency spectrums of signals in transmission line

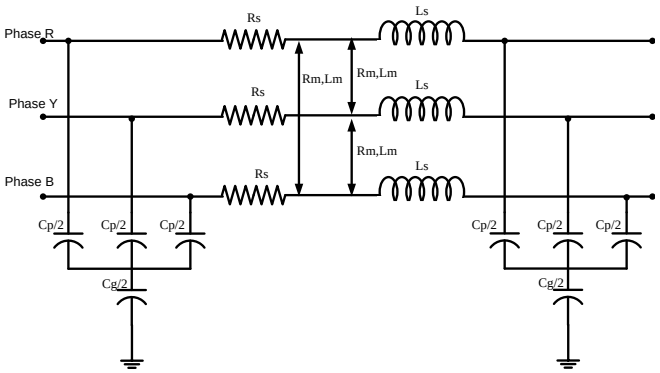

Fig. 2. Three phase balanced single PI transmission line model with lumped parameters

are small, the frequency independent line parameters would give accurate solution.

$$\lambda = \frac{v}{f} \tag{1}$$

Where, λ is wave lengths of voltage ($V_{(x,t)}$) and current ($I_{(x,t)}$), υ is velocity of wave propagation, and f is frequency of wave.

2.1. Single PI section balanced 3-Phase Line Model

A common representation of 3-phase PI transmission line model has shown in Fig. 2. It is an approximation of distributed parameters line model, i.e. it will become obviously reference to the exact decoupled propagation wave based transmission line model. The equivalent line parameters of this line model are derived as the product of per kilometer parameter and line length (x). However, if the line length is more than 60km, the line parameters are computed using hyperbolic correction factors. The equivalent impedance and admittance matrixes of this line are calculated at 50Hz frequency. Therefore, based on the line parameters, the line described as a balanced 3-phase line, it does not include effect of corona and transposition of line is not possible. By considering the transmission line length (x) and p.u parameters [32] of the line, the computation of PI transmission line parameters are as follows (Fig. 2): If the line length is <60Km, the hyperbolic correction factors would be equal to 1. Therefore, the effect of the characteristic impedance is small or negligible, but in these the load impedance was dominated. The equivalent sequence parameters are calculated as follows:

$$R_1 = r_1 \; x \; h_{r1} \tag{2a}$$

$$L_1 = l_1 \; x \; h_{l1} \tag{2b}$$

$$C_1 = c_1 \; x \; h_{c1} \tag{2c}$$

$$R_0 = r_0 \; x \; h_{r0} \tag{3a}$$

$$L_0 = l_0 \; x \; h_{l0} \tag{3b}$$

$$C_0 = c_0 \; x \; h_{c0} \tag{3c}$$

Where, R_1, L_1, and C_1 are equivalent positive sequence transmission line resistance, inductance, and capacitance parameters respectively. Similarly, R_0, L_0, and C_0 are equivalent zero sequence transmission line resistance, inductance and capacitance respectively. The Eq. (2) and Eq. (3) are using to derive the equivalent lumped parameters of the line as follows:

$$R_s = \frac{(2R_1 + R_0)}{3} \tag{4a}$$

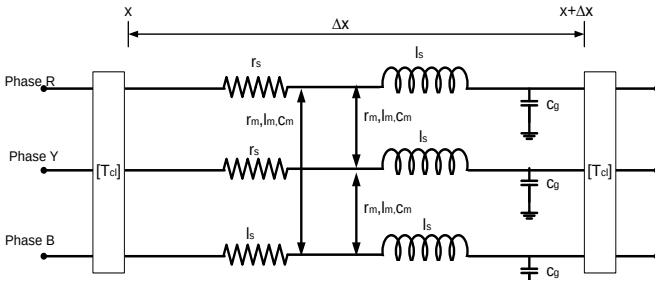

Fig. 3. Schematic representation of three phase distributed transmission line model with distributed parameters

$$L_s = \frac{(2L_1 + L_0)}{3} \tag{4b}$$

$$C_p = C_1 \tag{4c}$$

$$R_m = \frac{(R_0 - R_1)}{3} \tag{5a}$$

$$L_m = \frac{(L_0 - L_1)}{3} \tag{5b}$$

$$C_g = \frac{3C_1C_0}{(C_1 - C_0)} \tag{5c}$$

Where, the 's' stands for self, the 'm' stands for mutual, the 'p' stands for phase and the 'g' stands for ground are indexing equivalent transmission line parameters. If the line length is $>$ 60Km, there would be a considerable change in hyperbolic correction factors. The computations of these factors are as follows, the p.u positive sequence impedance (z_1) and admittance (y_1) are

$$z_1 = (r_1 + jwl_1) \tag{6a}$$

$$y_1 = (g_1 + jwg_1) \tag{6b}$$

Where$w = 2\pi f$, the characteristic impedance is dominating in long lines. Therefore, the per km positive sequence characteristic impedance (Z_{c1}) and propagation constant (γ_1) are derived as follows:

$$Z_{c1} = \sqrt{\frac{z_1}{y}}_1 \tag{7}$$

$$\gamma_1 = \sqrt{z_1 \, y_1} \tag{8}$$

The equivalent PI line positive sequence Z_1 and Y_1 are described as,

$$Z_1 = (R_1 + jwL_1) = Z_{c1} \sinh(\gamma_1 . x) \tag{9}$$

$$Y_1 = (G_1 + jwC_1) = \frac{2}{Z_{c1}} \tanh(\gamma_1 . \frac{x}{2}) \tag{10}$$

Similarly, Z_0 and Y_0 are also calculated by using Eq. 6 to Eq. (10). Finally, the equivalent PI line parameters are also obtained by using Eq. (4) and Eq. (5). In long transmission lines the correction factors increases Z and decreases Y. As shown in Eq. (11), the $[Z]$ and $[Y]$ matrices are described a balanced 3-phase transmission line with equal self and mutual elements.

$$[Z] = \begin{bmatrix} Z_s & Z_m & Z_m \\ Z_m & Z_s & Z_m \\ Z_m & Z_m & Z_s \end{bmatrix}, [Y] = \begin{bmatrix} Y_s & Y_m & Y_m \\ Y_m & Y_s & Y_m \\ Y_m & Y_m & Y_s \end{bmatrix} \tag{11}$$

The solution of voltage and current in PI line model is obtained from Eq. (12) and Eq. (13).

$$[V_s] = \left([I] + \frac{[Z][Y]}{2}\right)[V_r] + [Z][I_r] \tag{12}$$

$$[I_s] = [Y]\left([I] + \frac{[Z][Y]}{4}\right)[V_r] + \left([I] + \frac{[Z][Y]}{2}\right)[I_r] \tag{13}$$

2.2. 3-Phase CP Line Model with Exact Decoupling

The Fig. 3 shows the incremental line segment of CP line of length varying from x to x+Δx. The solution of the 3-phase CP line model in EMTP was obtained from Clarke's transformation. In this method first the solution was performed in model domain, after that it was transformed back to original domain to interact with the remaining network. The solution of normal CP line model cannot describe as complete decoupled line due to mutual terms. The present work is concentrated to remove these terms and achieve good approximation of modes of transmission line in the way of adequate frequency independent transformation. To eliminate mutual terms, the line model is considered as transposed and vertical symmetry to get accurate solution and complete decoupled modes.

When the line is excited by using a constant frequency (w) a.c source, the phase voltage (V_{ph}) and current (I_{ph}) equations of a 3-phase CP line [7], [12], [14], and [23] are specified as follows:

$$\frac{d[V_{ph}]}{dx} = -[Z][I_{ph}] \tag{14a}$$

$$\frac{d[I_{ph}]}{dx} = -[Y][V_{ph}] \tag{14b}$$

As shown in Fig. 3, the variables of $[Z]$ and $[Y]$ are given for per unit line length. The mutual terms of these matrices do not give a trivial solution, therefore the second derivative of Eq. (14) is on the back substitution.

$$\frac{d^2[V_{ph}]}{dx} = [Z][Y][V_{ph}] \tag{15a}$$

$$\frac{d^2[I_{ph}]}{dx} = [Y][Z][I_{ph}] \tag{15b}$$

Where, in model domain the voltage $[\hat{V}]$ and current $[\hat{I}]$ equations are related by transformation matrixes T_v and T_i.

$$\left[\hat{V}\right] = \left[T_v{}^{-1}\right][V_{ph}] \tag{16a}$$

$$\left[\hat{I}\right] = \left[T_i{}^{-1}\right][I_{ph}] \tag{16b}$$

Substitute Eq. (16) in Eq. (15). Generally, $[Z]$ and $[Y]$ are symmetric matrices. If these matrices are frequency independent, The T_i and T_v are also frequency independent.

$$\frac{d^2\left[\hat{V}\right]}{dx} = [T_v^{-1}][Z][Y][T_v]\left[\hat{V}\right] \tag{17a}$$

$$\frac{d^2\left[\hat{I}\right]}{dx} = [T_i^{-1}][Y][Z][T_i]\left[\hat{I}\right] \tag{17b}$$

From Eq. (17), the eigenvalues of $[Z][Y]$ and $[Y][Z]$ are identical. Therefore voltage and current would give the same modes of propagation, but the eigen vectors are different and related as,

$$T_i = \left(T_v^t\right)^{-1} \tag{18}$$

Also, substitute Eq. (16) in Eq. (15). Therefore the first order differential equations in model domain are as follows,

$$\frac{d\left[\hat{V}\right]}{dx} = -[T_v^{-1}][Z][T_i]\left[\hat{I}\right] \tag{19a}$$

$$\frac{d\left[\hat{I}\right]}{dx} = -[T_i^{-1}][Y][T_v]\left[\hat{V}\right] \tag{19b}$$

The Eq. (17) and Eq. (19) are transformed the 3-phase transmission line in to decoupled set of modes. The model impedance ($[\hat{Z}]$) and admittance ($[\hat{Y}]$) matrices are as,

$$\left[\hat{Z}\right] = [T_v^{-1}][Z][T_i]\,,\left[\hat{Y}\right] = [T_i^{-1}][Y][T_v] \tag{20}$$

The CP line is using the Clarke's transformation matrix (T_{cl}) to obtain decoupling of lines in model domain.

$$[T_{cl}] = \begin{bmatrix} \frac{1}{\sqrt{3}} & \frac{1}{\sqrt{2}} & \frac{1}{\sqrt{6}} \\ \frac{1}{\sqrt{3}} & -\frac{1}{\sqrt{2}} & \frac{1}{\sqrt{6}} \\ \frac{1}{\sqrt{3}} & 0 & -\frac{2}{\sqrt{6}} \end{bmatrix} \tag{21}$$

In non-transposed line T_v and T_i are different, because each mode has its own characteristic impedance (Z_c) and propagation constant (γ). Therefore, the solution of the $[\hat{Z}]$ and $[\hat{Y}]$ matrices are consisting of $Z_{\alpha 0}$ and $Y_{\alpha 0}$ elements [11], [12], [14], [18], [23]. In this paper, the $[Z]$ and $[Y]$ matrixes are computed at 50Hz frequency and also considered continuously transposition of lines. Therefore, the solution of $[[\hat{Z}]]$ and $[[\hat{Y}]]$ matrix does not consist of any mutual elements and lines are completely decoupled.

$$\left[\hat{Z}\right] = \begin{bmatrix} Z_0 & 0 & 0 \\ 0 & Z_\alpha & 0 \\ 0 & 0 & Z_\beta \end{bmatrix}, \left[\hat{Y}\right] = \begin{bmatrix} Y_0 & 0 & 0 \\ 0 & Y_\alpha & 0 \\ 0 & 0 & Y_\beta \end{bmatrix} \tag{22}$$

The accuracy and frequency response of these transmission line models are verified by designing 3-phase IEEE 57 test case system with proposed transmission line models.

The Fig.4 shows the single phase positive equivalent circuit of the IEEE 57 bus power system network. By using the standard test case network data [31], 3-phase power system networks are designed by PI and CP transmission line models in Matlab and EMTP-RV respectively. The transmission lines are modeled by using the standard per km sequence parameters of 138 kv line [32], the positive sequence parameters are r_1=0.12 Ω/km, l_1=1.52 mH/km, and c_1=0.0087 F/km. Similarly, the negative sequence parameters are r_0=0.36 Ω/km, l_1=4.905 mH/km, and c_0=0.0056 F/km. The power system was consisted 63 transmission lines, among all those lines the minimum line length was described as 1.51km and maximum line length was described as 117.04km. While modeling the power system with PI lines, some of the lines had length greater than 60km i.e. yellow squares shown in Fig. 4, only these lines were accounted by hyperbolic correction factors during computation. However, in these line models the effect of corona and its losses are not considered, unless it is cascaded by number of PI sections. When compared with PI line model, the transmission line parameters are accurately accounted in distributed CP line model. While modeling the power system with these lines, the line parameters were calculated at 50Hz frequency based on its transmission line length. In addition to that while designing power system with these lines, each line is continuously transposed so that the model transformation solution of the 3-phase line with 3 conductors was found as T_i=T_v and $[\hat{Z}][\hat{Y}]$= $[\hat{Y}][\hat{Z}]$. This relation describe that the CP line was exactly decoupled on both sides of transmission line in power system network. All generator buses in this power system are excited by a.c voltage of 138 kv at 50Hz frequency. Therefore, the frequency spectrum of voltage and current waves are narrow range in transmission lines. Because of this property and proposed conditions the CP line system was given accurate results and fast solution.

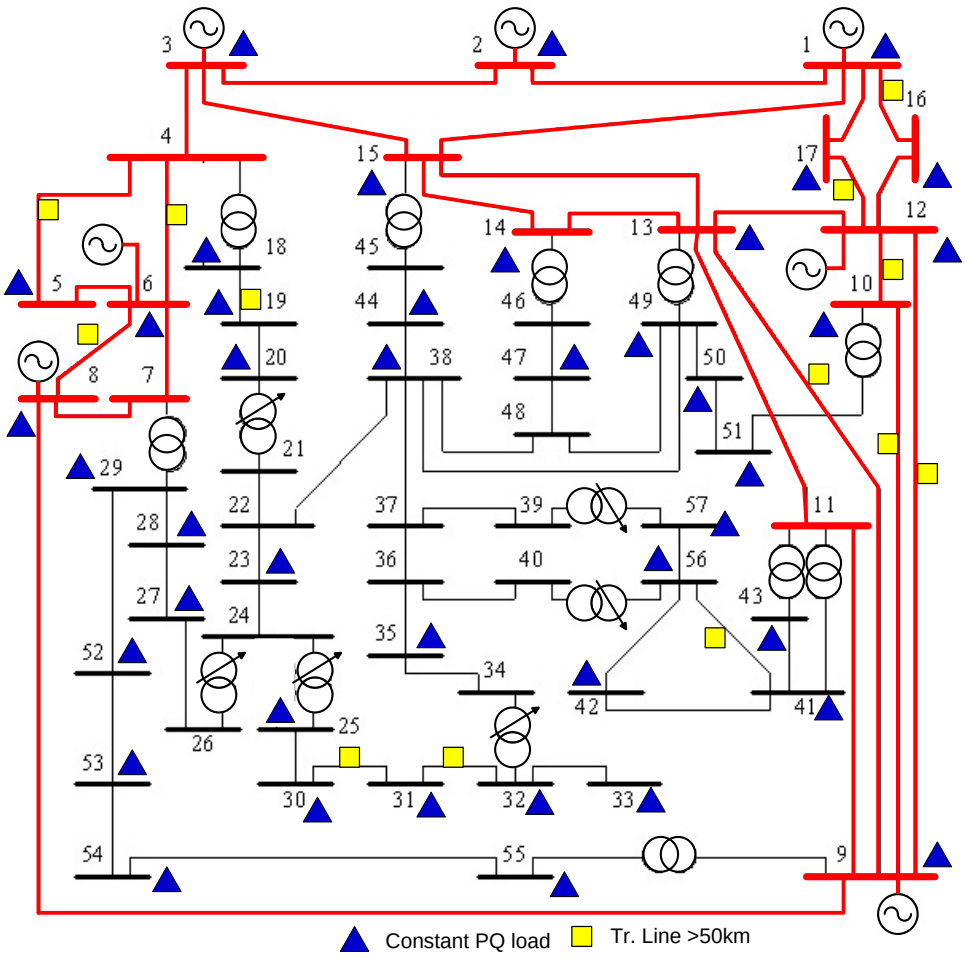

Fig. 4. Single phase positive sequence connection diagram of IEEE 57 bus power system

3. Optimization Problem Formulation

A non-linear constraints based power loss objective function is described for minimizing of power system losses for optimization of proposed power system models. The mathematical formulation of minimization of power system loss is defined to set control variables, such as generator bus voltages, tap setting of transformers and shunt capacitors. The constrained optimization problem is like:

$$Min\, F(x,u) \tag{23}$$

Where, the minimizations of transmission losses are subjected to equality (g(x,u)=0) and inequality (h(x,u)) constraints to define optimization objective function.

$$subjected\, to: \begin{cases} g(x,u)=0 \\ h(x,u)_{\min} \le h(x,u) \le h(x,u)_{\max} \end{cases} \tag{24}$$

x: is a vector of control variables, such as bus voltages (V_{bi}), generator absolute power (S_{gi}) and transmission line absolute power (S_{ti}).

$$x = [V_b \cdots\cdots V_{bi}, S_g \cdots\cdots S_{gi}, S_t \cdots\cdots S_{ti}] \tag{25}$$

u: is a vector of independent variables, such as generator voltages (V_g), tap-setting of transformer (T_a), and capacitor banks (Q_c).

$$u = [V_g \cdots\cdots V_{gi}, T_a \cdots\cdots T_{ai}, Q_c \cdots\cdots Q_{ci}] \tag{26}$$

3.1. Objective Functions

In this paper the objective function is described by using three functions as follows:

- F_1= Min (total power loss in transmission lines).
- F_2= Min (Voltage deviation).
- F_3= Min (Max (Voltage stability index)).

A) Power Loss Minimization (P_{loss})

The minimization of power loss is described based on the optimal adjustment of control parameters ((25)). It is defined as follows:

$$F_1(x,u) = \min\Big(\sum_{l=1}^{no.of\ lines} Y_l(V_p^2 + V_q^2 - 2\ V_p V_q\ \cos\ \theta_{pq}\Big) \tag{27}$$

Where, Y_l is the line admittance, V_p is from bus voltage, V_q is to bus voltage, and θ_{pq} is admittance angle.

B) Voltage deviation (VD)

This function is used observes the violation of voltage deviation (VD) of all transmission lines. The minimization of this function was obtained by summing absolute deviations of all lines. It is derived as,

$$F_2(x,u) = \min \sum_{k=1}^{no.of\ line} \left| V_p - V_p^{ref} \right| \tag{28}$$

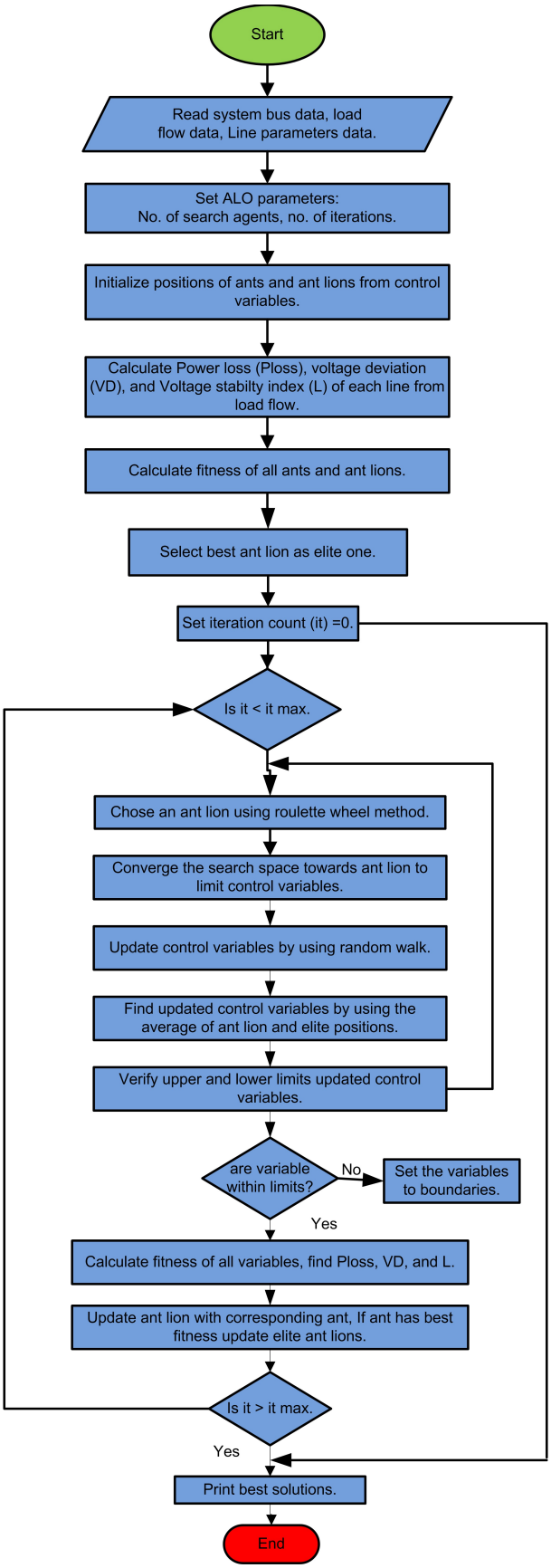

Fig. 5. Flow chart of proposed ALO

C) Voltage stability index (L)

The study of this function gives sufficient information about the voltage stability index (VSI) of proposed systems and reports the voltage collapse information of power system.

$$F_3(x,u) = \min\left(\max(L_j)\right) \tag{29}$$

Where, L_j is the stability index of each transmission line.

$$L_j = \left| 1.0 - F_{pq}\,\frac{V_p}{V_j}\angle\theta_{pq} + \delta_p - \delta_q \right| \tag{30}$$

Where, $F_{pq} = -[Y_1]^{-1}\,[Y_2]$. The Y_1 and Y_2 are sub matrices, they were defined from the transmission lines connected between buses as shown in Eq. (31).

$$\begin{bmatrix} I_p \\ I_q \end{bmatrix} = \begin{bmatrix} Y_1 & Y_2 \\ Y_3 & Y_4 \end{bmatrix} \begin{bmatrix} V_p \\ V_q \end{bmatrix} \tag{31}$$

3.2. 3.2. Constraints

A) Equality constraints

$$P_{gi} - P_{di} - \sum_{l=1}^{no.of\,lines} V_p\,V_q\,Y_l\,\cos\left(\theta_{pq} - \delta_p + \delta_q\right) = 0 \tag{32}$$

$$Q_{gi} - Q_{di} - \sum_{l=1}^{no.of\,lines} V_p\,V_q\,Y_l\,\sin\left(\theta_{pq} - \delta_p + \delta_q\right) = 0 \tag{33}$$

B) Inequality constraints

- Generator constraints

$$V_{gi}^{\min} \le V_{gi} \le V_{gi}^{\max} \quad gi = 1,2,...ng \tag{34}$$

$$Q_{gi}^{\min} \le Q_{gi} \le Q_{gi}^{\max} \quad gi = 1,2,...ng \tag{35}$$

- Tap setting constraints

$$T_i^{\min} \le T_i \le T_i^{\max} \quad i = 1,2...nt \tag{36}$$

- Shunt capacitor compensation

$$Q_{ci}^{\min} \le Q_{ci} \le Q_{ci}^{\max} \quad i = 1,2...ci \tag{37}$$

In this paper, the control variables of x are self-constrained, but the state variable are constrained by using the penalty function. To discard any unfeasible solution the modified objective function is derived as follows.

$$P_{loss} = F(x,u) + \lambda_v\,\Delta {V_{gi}}^2 + \lambda_g\,\Delta {S_{gi}}^2 + \lambda_{tp}\,\Delta {T_{tp}}^2 \tag{38}$$

Where, λ_v , λ_g, and λ_{tl} are the penalty factors of dependent variables.

$$\Delta V_{gi} = \begin{cases} (V_{gi}^{\min} - V_{gi})\ if\ V_{gi} \le V_{gi}^{\min} \\ (V_{gi} - V_{gi}^{\min})\ if\ V_{gi} \ge V_{gi}^{\max} \\ 0\ if\ V_{gi}^{\min} \le V_{gi} \le V_{gi}^{\max} \end{cases} \tag{39}$$

$$\Delta S_{gi} = \begin{cases} (S_{gi}^{\min} - S_{gi})\ if\ S_{gi} \le S_{gi}^{\min} \\ (S_{gi} - S_{gi}^{\min})\ if\ S_{gi} \ge S_{gi}^{\max} \\ 0\ if\ S_{gi}^{\min} \le S_{gi} \le S_{gi}^{\max} \end{cases} \tag{40}$$

$$\Delta T_{tpi} = \begin{cases} (T_{tpi}^{\min} - T_{tpi})\ if\ T_{tpi} \le T_{tpi}^{\min} \\ (T_{tpi} - T_{tpi}^{\max})\ if\ T_{tpi} \ge T_{tpi}^{\max} \\ 0\ if\ T_{tpi}^{\min} \le T_{tpi} \le T_{tpi}^{\max} \end{cases} \tag{41}$$

4. ANT LION OPTIMIZATION ALGORITHM (ALO)

The Ant Lion Optimization (ALO) is one of the meta-heuristic algorithms. It was introduced by Seydali Mirjalili [27] to salve constrained optimization engineering problems. It is termed as best global optimizer, because it can achieve balance between exploration and exploitation to yield high probability by avoiding stagnation in local optima and hence guarantees the best convergence. Basically, the ALO shows mimics of hunting behavior of the ant lions in nature. Generally, at larva stage the ant lions were made pits for hunting the ants. When the ants are searching for food in a stochastic moment manner, the ant lions sense disturbance and eat them. The behavior of interaction between ant and ant lion is described mathematically in ALO.

Initially, number (n) of ants and ant lions, dimension of search space (d) with upper and lower bonds, and maximum number of iterations are supposed to be initialized. Likewise, power system data has to be specified in algorithm. In the present problem ant and ant lions are described as solution vectors and position of ants in predefined search space. The vector i.e Eq. (26) was consisted control variables, these variables are initialized randomly and specified in M_{ant} matrix during optimization.

$$M_{ant} = A(i,j) = \begin{bmatrix} A_{11} & A_{12} & \cdots & A_{1d} \\ A_{21} & A_{22} & \cdots & A_{2d} \\ \vdots & \vdots & \ddots & \vdots \\ A_{n1} & A_{n2} & \cdots & A_{nd} \end{bmatrix} \tag{42}$$

The Eq. (42) shows the positions of n number of ants in d dimensional search space. Similarly, ant lions are hidden somewhere in the search space. The $M_{ant\ lion}$ matrix is derived same as M_{ant} matrix as follows.

$$M_{antlion} = \begin{bmatrix} Al_{11} & Al_{12} & \cdots & Al_{1d} \\ Al_{21} & Al_{22} & \cdots & Al_{2d} \\ \vdots & \vdots & \ddots & \vdots \\ Al_{n1} & Al_{n2} & \cdots & Al_{nd} \end{bmatrix} \tag{43}$$

However, the position of ant and ant lions within the search space is described by using following equation:

$$A_{ij} = A_{ij}^{lower} + rand(A_{ij}^{upper} - A_{ij}^{lower}) \tag{44}$$

The fitness function was shown evaluation of ant and ant lions by using the Eq. (38), it was described best fitness ant lion from the given function. The roulette wheel method is using for select best fitness of ant lion. This method shows more probability to eat ants by building ant lion traps in search space. After selecting the ant lions, the boundaries for control variables have updated by limiting the search space in order to decrease the random walk of ants. The new position of ants tends to move around the best fitness ant lion. It is derived as follows:

$$c_i^t = antlion_j^t + c^t \tag{45}$$

$$d_i^t = antlion_j^t + d^t \tag{46}$$

Where, $c^t{}_i$ is minimum of all variable at iteration t, $d^t{}_i$ is maximum of all variables of i^{th} ant in vector, and $antlion^t{}_i$ is position of j^{th} ant at i^{th} iteration. When the ant is going for searching food, the random walk of ant was like stochastic nature. The random walk of ant is expressed as follows:

$$X(t) = [0, cum\,sum(2r(t_1) - 1),\ cum\,sum(2r(t_2) - 1), \\ .....cum\,sum(2r(t_n) - 1),] \tag{47}$$

Where, X(t) is random walk of ants, n is no. of iterations, t is time step of random walk, and r(t) is stochastic function. The r(t) is defined as follows:

$$r(t) = \begin{cases} 1\ if\ rand > 0.5 \\ 0\ if\ rand \leq 0.5 \end{cases} \tag{48}$$

Where, rand is the number uniformly distributed in the range 0 and 1.When the ants are moving randomly, in each step the position of ants were update b to a in random search space i.e Eq. (**??**). The new positions of ants are derived by the following equation.

$$X_i^t = \frac{(X_i^t - a_i)\,x\,(d_i - c_i^t)}{(d_i^t - a_i)} + c_i \tag{49}$$

The elitism phenomenon in ALO was helps to preserve and improved to the superior solution during entire optimization. The ants are not walk around roulette wheel selected ant lion only, simultaneously, they are also allowed to walk around elite ant lion. The average of two walks is considering defining new positions of ants.

$$ant_j^t = \frac{R_A^t + R_E^t}{2} \tag{50}$$

Where, $R_A^t$and R_E^t are roulette wheel ant lion and elite ant lion respectively at t^{th} iteration. Based on these mechanisms the ant lions are constructing pits based on fitness for catching ants. When the ant is sliding towards center of pit, the ant lion shot sand on it at the middle of trap. This mechanism explained as follows:

$$c^t = \frac{c^t}{I} \tag{51}$$

$$d^t = \frac{d^t}{I} \tag{52}$$

Where, I is the ratio. After this process, the new positions of ants obtained so far are verified with limiting values. If the position of ant was violated, it was restricted to with in the search space. Similarly, the fitness of ant is calculated based on the corresponding ant lion. If the new ant lion position is greater than the limits, the elite position of ant lion was selected among all iterations. The elite ant lion is selected for next iteration process. It is expressed mathematically as follows:

$$antlion_j^t = ant_j^t\ if\ f(ant_j^t) > f(antlion_j^t) \tag{53}$$

$$elite = antlion_j^t\ if\ f(antlion_j^t) > elite \tag{54}$$

If the current iteration is reached the specified maximum iterations, the present ant lion is displayed as the best optimal solution. The ALO optimization process is shown in Fig. 5.

5. PERFORMANCE ANALYSIS OF PROPOSED LINE MODEL POWER SYSTEMS.

This section presents the performance of proposed PI and CP transmission line models based time-domain power system models in terms of accuracy and frequency response. In addition to that this section verify the capability of these power system models by using the recently developed a well-known Ant Lion Optimization (ALO) algorithm.

The 3-phase NR load flow solution is used to assess the accuracy and frequency response of the proposed IEEE 57 bus systems. Each model has simulated by using balanced and unbalanced load flow studies. In these power systems PV buses are excited with the standard voltage of 1.06 p.u and slack bus is excited by 1.00 p.u at 50Hz frequency. All simulation results were compared with base case positive sequence load flow results. This section has discussed the transmission line error as function of the length, the frequency response of self and mutual parameters, and optimization of PI and CP lines power systems by using power loss minimization technique.

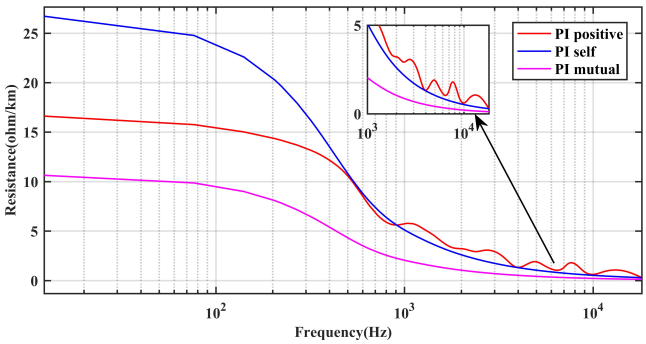

Fig. 6. Self and mutual resistance of the balanced PI lines systems

Table 1. Bus Voltage Magnitude Results – Balanced PQ Loads

Bus No.	Test case	PI line system	CP line system	Bus No.	Test case	PI line system	CP line system
1	1.04	1.00	1.00	30	0.96	1.00	0.97
2	1.01	1.00	1.00	31	0.94	0.99	0.96
3	0.99	1.00	1.00	32	0.95	1.00	0.98
4	0.98	0.99	0.98	33	0.95	1.00	0.98
5	0.98	0.99	0.97	34	0.96	0.98	0.96
6	0.98	1.00	1.00	35	0.97	0.99	0.96
7	0.98	0.99	0.98	36	0.98	0.99	0.97
8	1.01	1.00	1.00	37	0.98	1.00	0.98
9	0.98	1.00	1.00	38	1.01	1.02	1.00
10	0.99	0.99	0.97	39	0.98	1.00	0.98
11	0.97	0.98	0.96	40	0.97	0.99	0.96
12	1.02	1.00	1.00	41	1.00	1.02	1.00
13	0.98	0.97	0.95	42	0.97	1.01	0.99
14	0.97	0.96	0.94	43	1.01	1.02	1.00
15	0.99	0.98	0.95	44	1.02	1.02	0.99
16	1.01	0.99	0.97	45	1.04	1.03	0.99
17	1.02	0.98	0.96	46	1.06	1.06	1.03
18	1.00	1.02	1.00	47	1.03	1.04	1.01
19	0.97	0.99	0.97	48	1.03	1.04	0.98
20	0.96	0.98	0.96	49	1.04	1.06	0.98
21	1.01	1.02	1.00	50	1.02	1.04	1.03
22	1.01	1.02	1.00	51	1.05	1.05	1.04
23	1.01	1.02	0.99	52	0.98	1.00	1.00
24	1.00	1.01	0.98	53	0.97	0.99	1.00
25	0.98	1.02	0.98	54	1.00	1.02	1.03
26	0.96	0.97	0.94	55	1.03	1.05	1.06
27	0.98	0.99	0.98	56	0.97	1.03	1.00
28	1.00	1.00	1.00	57	0.96	1.02	0.99
29	1.01	1.02	1.02				

5.1. Balanced Power System with Balanced PQ Loads

This section discussed about the results of balanced load flow analysis, the PI lines system was converged in 3 iterations and the CP lines system was converged in 5 iterations. The EMTP simulation had shown less CPU time of 0.15625s, also the system was optimized to find load flow solution by moving quickly in to time domain initialization. The CP lines system was converged in more number of iterations; it is due to the more number of loops in the system. Based on variation of results, the Table 1 and Table 2 have described similar performance of both power systems models. Maximum approximation errors were observed as 6.10 % and 8.77 % in the positive sequence system and in the PI systems respectively at 49^{th} bus. The solution of parameters of $[\hat{Z}]$ and $[\hat{Y}]$ matrixes were shown increase in magnitudes, therefore the CP lines system was shown the large deviation of phase angle at all the buses. The largest phase angle was found 57.32° at 6^{th} bus.

5.2. Balanced Power System with Unbalanced PQ Loads

This section discuss about the results of unbalanced load flow analysis. Again, the PI lines system was converged in 3 iterations

Table 2. Bus Phase Angle Results – Balanced PQ Loads

Bus No.	Test case	PI line system	CP line system	Bus No.	Test case	PI line system	CP line system
1	0.00	0	0.00	30	-18.72	-14.6	33.50
2	-1.19	-1.89	13.91	31	-19.38	-15.62	30.76
3	-5.99	-7.38	33.65	32	-18.51	14.89	29.02
4	-7.34	-8.79	39.45	33	-18.55	-14.96	28.95
5	-8.55	-10.07	47.99	34	-14.15	-14.75	29.06
6	-8.67	-10.23	57.32	35	-13.91	-14.41	29.11
7	-7.60	-9.04	53.54	36	-13.64	-14.02	29.32
8	-4.48	-5.8	55.60	37	-13.45	-13.76	29.07
9	-9.59	-11.23	46.80	38	-12.74	-12.67	28.39
10	-11.45	-12.49	33.22	39	-13.49	-13.91	29.08
11	-10.19	-11.78	36.91	40	-13.66	-14.01	29.81
12	-10.47	-11.56	26.53	41	-14.08	-12.15	36.15
13	-9.80	-11.22	29.99	42	-15.53	-13.69	32.50
14	-9.35	-10.54	27.65	43	-11.35	-11.85	36.82
15	-7.19	-8.31	24.95	44	-11.86	-11.77	27.17
16	-8.86	-9.75	17.60	45	-9.27	-9.05	25.41
17	-5.40	-5.96	8.27	46	-11.12	-11.28	27.57
18	-11.73	-9.43	38.70	47	-12.51	-12.4	28.02
19	-13.23	-11.98	32.87	48	-12.61	-12.46	29.07
20	-13.44	-12.8	29.88	49	-12.94	-12.23	29.08
21	-12.93	-12.82	29.72	50	-13.41	-13.25	29.54
22	-12.87	-12.84	29.11	51	-12.53	-12.91	32.44
23	-12.94	-12.92	29.41	52	-11.50	-12.13	48.62
24	-13.29	-13.56	35.33	53	-12.25	-12.91	47.37
25	-18.17	-13.81	34.99	54	-11.71	-12.44	46.76
26	-12.98	-13.38	36.32	55	-10.80	-11.55	46.65
27	-11.51	-11.97	45.37	56	-16.07	-14.04	30.08
28	-10.48	-10.95	49.08	57	-16.58	-14.04	29.08
29	-9.77	-10.2	51.41			—	

and CP lines system was converged in 5 iterations. The EMTP simulation has shown the CPU run time is 0.10938s. The Table 3 was shown magnitude of voltage results on A, B, and C phases; from this table it was observed that the maximum approximation error is 3.98% at 45^{th} bus on phase C. The Table 4 shows phase angle of all three phases, the highest phase angle was found as 72.27o in CP lines system at bus 6 on phase C.

5.3. Transmission line error and Frequency response of Line parameters

This section is discussed about the effect of the transmission line length and corresponding frequency responses on the line parameters [19], [22], [23]. The PI line model used in the proposed power system was balanced, therefore the self (Z_s &Y_s) and mutual (Z_m &Y_m) terms of $[Z]$ and $[Y]$ matrices were equal in magnitudes. When this transmission line model was used to design power system in this paper, the response of the proposed power system had shown similar to the low pass filter. Therfore, beyond the cut-off frequency the voltage and current waves were attenuated in this proposed system as shown in Fig. 6 and Fig. 8. Whereas in the CP lines power system the line parameters had continuously transposed, the solution of $[\hat{Z}]$ and $[\hat{Y}]$ matrices was described that this power system transmission lines were operating in α=β mode and 0 mode only (i.e. two modes only). These two modes results this power system response was like the high pass filter. As shown in Fig. 7 and Fig. 9, this power system model had the upper cut-off frequency of 1.2 kHz; it was shown that this power system model was performed satisfactorily to the high frequency voltage and current waves only. Whereas for the low frequency disturbances, the PI lines system gives accurate results, but for transient disturbances the CP lines system gives accurate results. The Fig. 6 is showing smooth variation of R_s, R_m and R_1 at lower frequencies in PI lines system.

The Fig. 7 is showing varation of resistance in CP line interms of mode-0 and mode-1 components at high frequencies. At lower frequencies the resistance parameters in this line is showing

Table 3. Bus Voltage Magnitude Results – Unbalanced PQ Loads – With Constant Voltage Sources

Bus	Phase-A		Phase-B		Phase-C	
	PI line system	CP line system	PI line system	CP line system	PI line system	CP line system
1	1.00	1.00	1.00	1.00	1.00	1.00
2	1.00	1.00	1.00	1.00	1.00	1.00
3	1.00	1.00	1.00	1.00	1.00	1.00
4	1.00	0.98	0.99	0.98	0.99	0.98
5	1.00	0.98	1.00	0.97	0.99	0.97
6	1.00	1.02	1.00	0.99	1.00	0.99
7	0.99	0.98	0.99	0.98	0.98	0.97
8	1.00	1.00	1.00	1.00	1.00	1.00
9	1.00	1.00	1.00	1.00	1.00	1.00
10	0.99	0.97	0.99	0.97	0.98	0.97
11	0.99	0.96	0.98	0.96	0.98	0.95
12	1.00	1.00	1.00	1.00	1.00	1.00
13	0.98	0.95	0.97	0.94	0.96	0.94
14	0.98	0.94	0.96	0.93	0.95	0.93
15	0.99	0.95	0.98	0.95	0.97	0.95
16	1.00	0.97	0.99	0.97	0.98	0.97
17	0.99	0.97	0.98	0.96	0.98	0.96
18	1.02	1.01	1.02	1.00	1.02	1.00
19	1.01	0.98	1.00	0.97	0.99	0.96
20	1.00	0.97	0.98	0.95	0.97	0.95
21	1.04	1.01	1.03	0.99	1.01	0.99
22	1.04	1.01	1.03	0.99	1.01	0.99
23	1.04	1.01	1.03	0.99	1.01	0.99
24	1.03	1.00	1.02	0.98	1.00	0.97
25	1.03	1.00	1.01	0.98	1.00	0.97
26	0.99	0.96	0.98	0.94	0.96	0.93
27	1.01	0.99	1.00	0.97	0.98	0.97
28	1.01	1.01	1.01	1.00	1.00	0.99
29	1.02	1.02	1.01	1.01	1.01	1.01
30	1.03	0.99	1.01	0.97	0.98	0.96
31	1.02	0.99	1.00	0.96	0.97	0.95
32	1.03	1.00	1.01	0.97	0.99	0.97
33	1.03	1.00	1.01	0.97	0.98	0.97
34	1.01	0.98	0.99	0.95	0.96	0.95
35	1.01	0.98	0.99	0.96	0.97	0.95
36	1.02	0.98	1.00	0.96	0.98	0.96
37	1.02	0.99	1.00	0.97	0.99	0.97
38	1.04	1.01	1.03	0.99	1.01	0.99
39	1.02	0.99	1.00	0.97	0.98	0.97
40	1.01	0.98	0.99	0.96	0.97	0.95
41	1.04	1.01	1.03	1.00	1.02	1.00
42	1.04	1.00	1.02	0.99	1.00	0.98
43	1.03	1.00	1.03	1.00	1.02	1.00
44	1.04	1.00	1.03	0.99	1.01	0.99
45	1.04	1.00	1.03	0.99	1.02	0.99
46	1.07	1.04	1.06	1.03	1.05	1.03
47	1.06	1.02	1.04	1.01	1.03	1.01
48	1.06	1.02	1.04	1.01	1.03	1.01
49	1.07	1.04	1.06	1.03	1.05	1.03
50	1.06	1.03	1.05	1.02	1.04	1.02
51	1.07	1.04	1.06	1.04	1.05	1.04
52	1.01	1.01	1.00	1.00	0.99	1.00
53	1.01	1.01	1.00	1.00	0.99	0.99
54	1.03	1.03	1.03	1.02	1.02	1.02
55	1.06	1.06	1.06	1.06	1.06	1.06
56	1.05	1.02	1.03	0.99	1.01	0.99
57	1.04	1.01	1.02	0.99	1.00	0.99

Table 4. Bus Phase Angle Results – Unbalanced PQ Loads – With Constant Voltage Sources

Bus	Phase-A		Phase-B		Phase-C	
	PI line system	CP line system	PI line system	CP line system	PI line system	CP line system
1	0.00	0.00	-120.00	-120.00	120.00	120.00
2	-1.27	13.91	-122.13	-106.09	117.26	133.91
3	-4.56	36.96	-127.66	-83.02	109.75	156.49
4	-5.39	39.52	-128.96	-80.50	107.67	159.34
5	-5.82	48.07	-130.23	-71.94	105.52	167.85
6	-5.58	57.31	-130.45	-62.69	105.04	177.31
7	-4.07	53.64	-129.15	-66.35	105.80	173.31
8	-0.44	55.60	-126.26	-64.41	109.08	175.59
9	-6.14	46.80	-131.42	-73.21	103.60	166.79
10	-7.88	33.32	-132.43	-86.67	102.54	152.98
11	-7.38	37.04	-131.67	-82.93	103.41	156.59
12	-7.05	26.53	-131.74	-93.48	103.86	146.51
13	-7.30	30.19	-131.08	-89.84	104.43	149.61
14	-7.07	27.91	-130.35	-92.16	105.50	147.18
15	-5.52	25.14	-128.24	-94.93	108.59	144.64
16	-6.40	17.79	-129.70	-102.33	106.64	137.32
17	-4.11	8.47	-125.85	-111.63	111.99	127.95
18	-5.98	38.80	-129.60	-81.26	106.97	158.53
19	-8.32	33.23	-131.72	-86.88	103.77	152.23
20	-9.05	30.33	-132.39	-89.80	102.69	149.08
21	-9.06	30.18	-132.40	-89.96	102.67	148.92
22	-9.05	29.57	-132.41	-90.56	102.61	148.30
23	-9.11	29.88	-132.49	-90.26	102.49	148.58
24	-9.36	35.83	-133.03	-84.26	101.32	154.38
25	-9.59	35.51	-133.28	-84.60	101.04	154.02
26	-9.17	36.80	-132.85	-83.26	101.48	155.39
27	-7.23	45.71	-131.74	-74.35	102.72	164.74
28	-6.04	49.32	-130.91	-70.73	103.79	168.64
29	-5.18	51.58	-130.30	-68.47	104.59	171.10
30	-10.41	34.11	-133.89	-85.99	100.10	152.35
31	-11.51	31.49	-134.70	-88.63	98.90	149.36
32	-10.92	29.65	-134.14	-90.48	99.98	147.84
33	-10.99	29.59	-134.20	-90.55	99.90	147.75
34	-10.79	29.68	-134.00	-90.44	100.15	147.89
35	-10.47	29.69	-133.73	-90.43	100.58	148.02
36	-10.08	29.85	-133.42	-90.27	101.07	148.32
37	-9.87	29.59	-133.20	-90.54	101.42	148.12
38	-8.93	28.83	-132.28	-91.31	102.85	147.61
39	-10.01	29.62	-133.33	-90.51	101.22	148.10
40	-10.03	30.33	-133.43	-89.78	101.05	148.85
41	-7.75	36.33	-132.04	-83.69	103.03	155.79
42	-9.51	32.90	-133.21	-87.12	101.29	151.71
43	-7.45	36.96	-131.74	-83.02	103.34	156.49
44	-8.27	27.59	-131.44	-92.57	104.10	146.48
45	-6.13	25.63	-128.98	-94.47	107.71	145.05
46	-7.71	27.87	-131.08	-92.23	104.66	147.05
47	-8.69	28.06	-132.05	-92.07	103.23	146.94
48	-8.71	28.43	-132.12	-91.70	103.13	147.32
49	-8.23	29.40	-132.07	-90.71	103.33	148.63
50	-9.03	29.86	-132.97	-90.22	101.95	148.96
51	-8.29	32.59	-132.85	-87.46	102.12	152.15
52	-7.14	48.92	-131.91	-71.13	102.32	168.04
53	-7.93	47.72	-132.57	-72.34	101.41	166.69
54	-7.40	46.97	-132.33	-73.08	102.08	166.36
55	-6.43	46.67	-131.74	-73.36	103.25	166.60
56	-10.04	30.59	-133.46	-89.51	101.00	149.12
57	-10.11	29.63	-133.45	-90.51	101.08	148.09

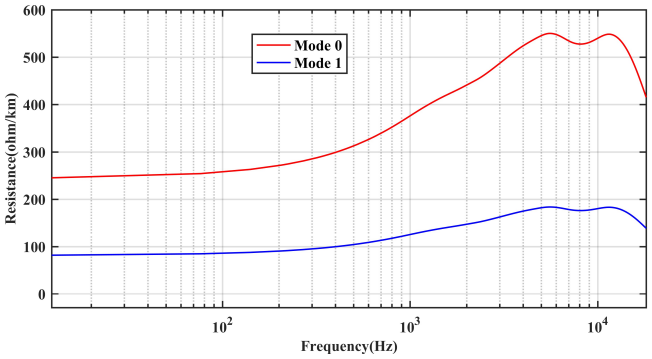

Fig. 7. Modes of resistance in transposed CP lines system.

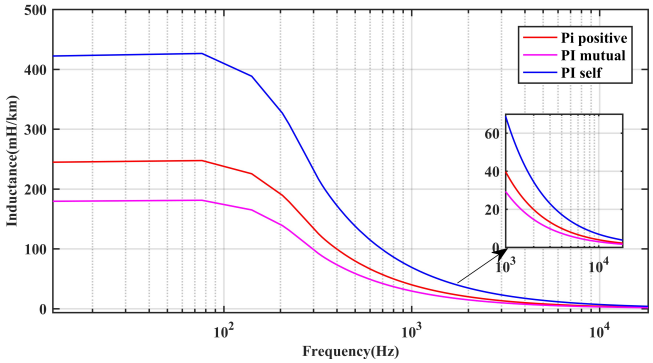

Fig. 8. Self and mutul inductance of the balanced PI lines system.

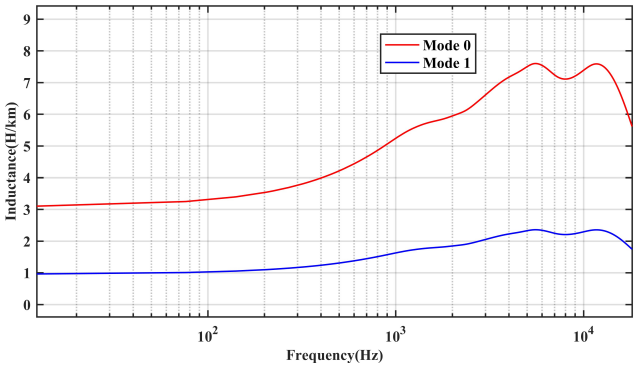

Fig. 9. Modes of inductance in transposed CPlines system.

constant magnitude, but for higher frequencies this line offers high impedance.

The Fig. 8 shows L_s, L_m and L_1 inductances are present only at lower frequencies. At these frequencies the parameter of PI lines had shown constant magnitude. But at higer frequencies i.e. above 1 kHz the inductances are almost negligible or zero.

When the inductance parameters was observed in CP line power system, based on the frequency of voltage and current wave forms the magnitude of modes of inductances were increasing. Beyond the maximum cut of frequency i.e. above 10 kHz, the magnitude was going to start decreasing.

The load flow simulation was carried out with the tolerance value of 10^{-4}. From the bus voltages the transmission line error is calculated based on maximum voltage described from the proposed models [23]. Proposed line models were derived by using frequency independent matrixes in this paper. In CP lines systems irrespective of line length the transmission lines were showing constant voltage error, but in PI lines system the error was increasing w.r.t line length. The Fig. 10 is showing voltage error of balanced power system models, the maximum error was found as 13.12% in CP lines system and 10.83% in PI lines systems in 17.22km transmission line, but in the single phase positive sequence system it was shown 13.26% in 49.30 km line. In PI lines systems when the line length was increasing, due to the lumped property of parameters of transmission line the voltage error was also increasing.

In the unbalanced load flow simulation also shown that the voltage error was constant in CP lines system irrespective of variation of transmission line length. But due to the variation of loads on the phases the percentage of voltage error was changing on A, B and C phases. Whereas the load on the three phases was different, the voltage errors were also different as shown in Fig. 11, Fig. 12 and Fig. 13. The maximum error was 13.49% at phase B in 17.22 km transmission line.

5.4. Minimization of power system losses

This section discusses about the optimization of proposed power system models by using three objective functions such as total power loss minimization (P_{loss}), voltage deviation (VD), and voltage stability index (L) techniques. Also, described the optimal setting of PV bus voltages (V_g) tap setting transformers (T) and setting of shunt capacitors (Q_c). The reliability and robustness of proposed power system models were verified by using ALO, GOT, WOT and SMO algorithms [27–30]. The Matlab simulations have performed by using "intel (R) core (TM) i5-5200 CPU @ 2.20 GHz 8 GB RAM" system. The IEEE 57 bus system consists of 7 generator variables, 17 tap setting transformer variables and 3 shunt capacitor variables. Including all objective functions with all control variables presented in Table 5.

In this paper all proposed models are used to optimize control variables by using the number of trials to achieve best optimal solutions. In this paper the minimization was achieved by using both continuous and discrete variables, these variables were initialized by using the randomization process. A penalty based minimization process was followed in this paper; this process convert constrained optimization problem into unconstrained problem. The penalty based solution is very necessary to get violation free solution of control variables. The normal trial and error method was used for select penalty factor [26], based on this method a low penalty factor 0.01 was obtained. Although it is very low, the sub optimal solution and violation of variables were omitted during optimization.

To show the effectiveness of proposed transmission line based power systems, the optimization process was executed for 50 trials and computed average optimum solution by using ALO, GOT, WOT and SMO algorithms. The P_{loss}, VD, L, and function run time was shown from Table 6 to Table 8.

A) Case 1: Positive sequence power system network.

Table 6 is showing optimal solutions of positive sequence power system. From the optimization results, it had found that the power loss was decreased by 6.9587%, voltage deviation (VD) was decreased by 0.176 p.u, and minimum voltage stability index (L)

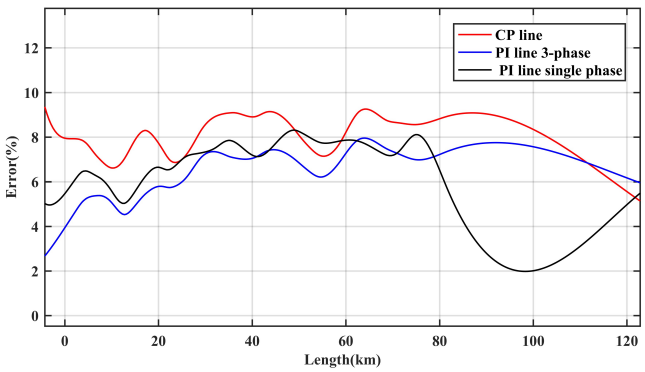

Fig. 10. Voltage error of balanced PI and CP lines power systems.

Table 5. Control Variables of Proposed Power Systems with Upper and Lower limits.

Control variables	Positive sequence system	3-phase PI lines system	CP lines system	Lower bond	Upper bond
Vg1	1.0400	1.0000	1.0000	0.94	1.06
Vg2	1.0100	1.0000	1.0000	0.94	1.06
Vg3	0.9850	1.0000	1.0000	0.94	1.06
Vg6	0.9800	1.0000	1.0000	0.94	1.06
Vg8	1.0050	1.0000	1.0000	0.94	1.06
Vg9	0.9800	1.0000	1.0000	0.94	1.06
Vg12	1.0150	1.0000	1.0000	0.94	1.06
T18	0.5155	0.5155	0.5155	0.90	1.10
T18	0.5112	0.5112	0.5112	0.90	1.10
T20	0.9588	0.9588	0.9588	0.90	1.10
T25	1.0000	1.0000	1.0000	0.90	1.10
T25	1.0000	1.0000	1.0000	0.90	1.10
T26	0.9588	0.9588	0.9588	0.90	1.10
T29	0.5171	0.5171	0.5171	0.90	1.10
T32	1.0256	1.0256	1.0256	0.90	1.10
T41	0.5236	0.5236	0.5236	0.90	1.10
T45	0.5236	0.5236	0.5236	0.90	1.10
T46	0.5556	0.5556	0.5556	0.90	1.10
T51	0.5376	0.5376	0.5376	0.90	1.10
T49	0.5587	0.5587	0.5587	0.90	1.10
T43	0.5219	0.5219	0.5219	0.90	1.10
T56	1.0438	1.0438	1.0438	0.90	1.10
T57	1.0204	1.0204	1.0204	0.90	1.10
T55	0.5319	0.5319	0.5319	0.90	1.10
Q18	2.1004	2.1004	2.1004	0.00	10.00
Q25	1.2392	1.2392	1.2392	0.00	5.90
Q53	1.3233	1.3233	1.3233	0.00	6.30
Total Power loss (p.u).	1.4481	18.2689	3.9676	n/a	n/a
Total Voltage deviation (VD). (p.u)	1.4200	0.8950	0.9470	n/a	n/a
Total Stability index (L).	0.9612	25.0282	57.1713	n/a	n/a

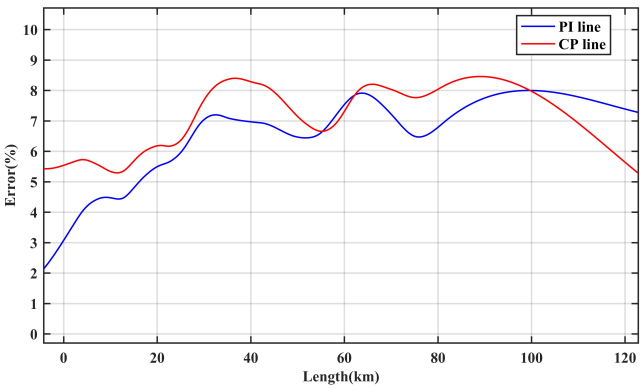

Fig. 11. Voltage error of Phase A of unbalanced PI and CP lines power systems.

was 0.208. For best optimization results, the objective function was executed in 2.35 seconds. When the ALO results are comparing with the other algorithm, the WOT was shown better results. It is due to the slow convergence while searching around the global optimum and less exploration capability, therefore without modifications and hybridization of this algorithm the results cannot described as best. Whereas, based on the large exploration of search space and fast convergence characteristics of ALO, it was efficiently handled control variables to give best optimization results. For best optimization results the generator voltages (V_g) was increased, the maximum voltage was 1.0454 p.u at bus 3 and minimum voltage was 1.0224 p.u at bus 1. Also, the tap setting of transformers were adjusted to the new positions, the maximum tap setting was 1.0692 p.u at 18 bus and minimum tap setting was 1.0254 at bus 20. The magnitude of shunt capacitors Q_{18} and Q_{25} were increased to 7.29395 p.u at bus 18 and 4.4678 p.u at bus 25respectively, but Q_{53} was decreased to 0.0087 p.u at bus 53.

Table 6. Comparison of Optimization Results of Positive Sequence Power System Network Variables

Control variables	ALO	GOT	WOT	SMO
Vg1	1.022451	1.01851	1.008422	1.00632
Vg2	1.028256	1.026323	1.0442	1.04335
Vg3	1.045483	1.014898	1.045619	1.011001
Vg6	1.042314	1.032871	1.020514	1.019904
Vg8	1.027345	1.021576	1.053762	0.98572
Vg9	1.029508	0.953684	1.053997	1.015643
Vg12	1.028233	0.991603	1.029954	1.019071
T18	1.069209	1.007725	1.060897	0.987631
T18	1.051354	1.006437	1.025318	0.998078
T20	1.025452	0.977931	1.06789	1.040038
T25	1.064374	1.029617	1.080614	0.986735
T25	1.046447	1.033552	1.073905	0.95256
T26	1.050432	0.974945	1.068873	0.82651
T29	1.044385	1.00777	1.084287	1.029867
T32	1.052847	1.012441	1.075422	0.957985
T41	1.051214	1.013443	1.064458	1.057793
T45	1.040989	1.014353	1.016456	0.952876
T46	1.025956	1.012573	1.099155	0.96102
T51	1.018316	0.994452	1.043133	1.055726
T49	1.055117	0.993329	1	0.92389
T43	1.055772	0.992805	1.053933	0.972801
T56	1.056979	1.012258	1.075559	0.958734
T57	1.043825	1.028631	1.052309	1.042703
T55	1.036308	0.992469	1.061309	0.978671
Q18	7.293953	8.934082	9.120294	-17.6278
Q25	4.467809	5.720677	5.224124	-5.25237
Q53	0.008739	0	0	0.539988
Power loss (p.u)	1.34733	1.336543	1.335295	4.368134
Voltage deviation (VD) (p.u)	0.17619	0.003889	0.133697	0.300249
Stability index (L)	0.208206	0.470564	0.175131	0.296752
Function runs time (seconds)	2.35	18.12158	0.47499	5.937404

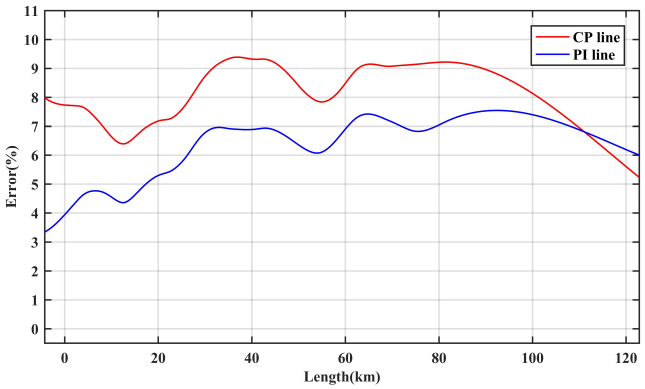

Fig. 12. Voltage error of Phase B of unbalanced PI and CP lines power systems.

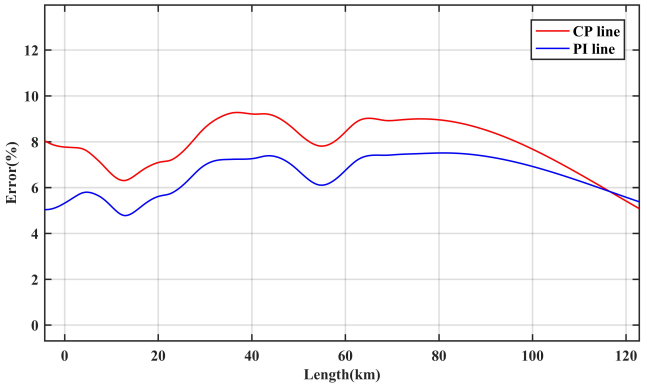

Fig. 13. Voltage error of Phase C of unbalanced PI and CP lines power systems.

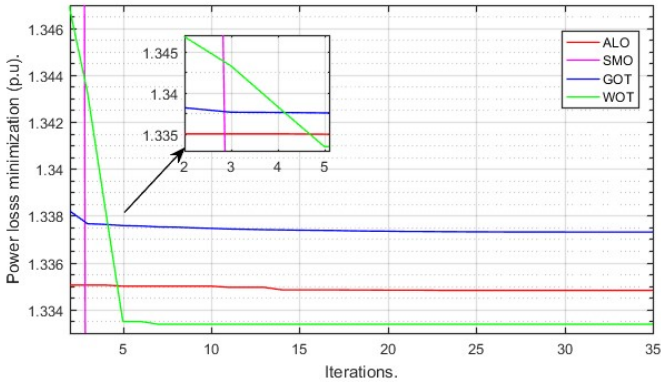

Fig. 14. Power loss minimizations in positive sequence power system network

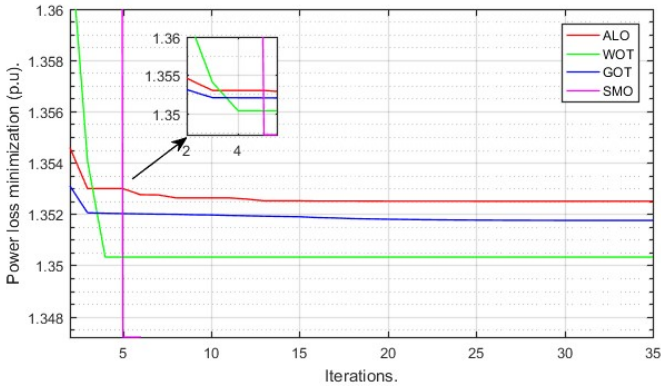

Fig. 15. Power loss minimizations in 3-phase PI lines power system network

Table 7. Comparison of Optimization Results of 3-Phase PI lines Power System Network Variables

Control variables	ALO	GOT	WOT	SMO
Vg1	1.027143	1.005204	1.022544	1.012058
Vg2	1.040605	1.004891	1.040177	1.002426
Vg3	1.031688	1.012058	1.041466	1.01379
Vg6	1.032408	1.027209	1.033702	0.991365
Vg8	1.032843	1.014846	1.040893	1.020228
Vg9	1.012821	0.997282	1.035955	0.973185
Vg12	1.033755	1.012795	1.047715	1.013989
T18	1.02559	1.012868	1.091419	0.962195
T18	1.039251	1.023982	1.066053	0.92479
T20	1.033228	0.999911	1.056262	0.945217
T25	1.035372	1.007851	1.05	1.012364
T25	1.016351	1.014455	1.028198	1.081572
T26	1.010572	0.948007	1.031581	0.952604
T29	1.030945	1.017323	1.06826	0.980014
T32	1.025608	1.014705	1.076119	1.027581
T41	1.033286	1.018495	1.0289	0.935678
T45	1.044009	0.996523	1.095102	1.069992
T46	1.01835	0.992772	1.053735	1.023194
T51	1.016261	0.984392	1.05	0.965126
T49	1.018466	1.02428	1.09428	0.978257
T43	1.030784	1.026808	1.074036	1.043826
T56	1.024059	1.001559	1.048103	0.965305
T57	1.052218	1.004741	1.071437	1.025246
T55	1.018458	1.021618	1.063974	0.938334
Q18	7.569781	9.172527	8.056226	-3.60733
Q25	3.46928	4.947151	4.350373	-0.04179
Q53	0.001826	0	0	-1.99754
Power loss. (p.u)	1.358283	1.353971	1.354581	0.717608
Voltage deviation (VD). (p.u)	0.251016	0.026082	0.027363	0.415534
Stability index (L).	0.053333	0.046945	0.104674	0.354312
Function runs time (seconds).	2.29	17.534	0.476011	6.0778

B) Case 2: 3-Phase PI lines power system network.

In this case the optimization results had shown considerable variation that was due to the increase in magnitude of line parameters. The Table 7 is summarized report of optimization results; the execution of objective function was in 2.29 seconds. When compared with execution time of case 1, this time was decreased. Similarly, the power loss was 1.358 p.u, but it was drastically decreased by 92.588 % that shows the adaptive shrinking mechanism nature of ALO to the specified boundaries. Due to the increase in line parameters in PI lines system, the voltage deviation (VD) was increased to 0.25 pu, but the voltage stability index (L) was greatly improved to 0.0533. Compared with case 1 results the generator voltages (V_g) are decreased in this optimization process, the maximum voltage was1.0406 p.u at bus 2 and the minimum voltage was 1.0128 p.u at bus 9. Also, the transformer tap settings were decreased, the maximum tap setting was 1.0522 at bus 57 and minimum tap setting was1.010 p.u at bus 26. Also, the Q18 was increased to 7.5697 p.u at bus 18, Q_{25} was decreased to 3.4692 p.u at bus 25 and also Q_{53} was decreased to 0.0018 p.u at bus 53.

C) Case 3: CP lines power system network.

The CP line power system mimics the behavior of actual power system, because the line parameters are uniformly distributed along the transmission line as shown in Fig. 3. In this model the total power system loss was greater than positive sequence power system and less than 3-phase PI lines power system. The optimization results are summarized in Table 8, the objective function was executed in 2.29 seconds and it is less execution time than case 1 and case 2 optimizations. The power loss of this system was 1.33 pu in ALO, it shows decrease of 66.23 % of power loss of this system. The voltage deviation (VD) in this system was increased to the 0.45 p.u, but the voltage stability was greatly improved to

Table 8. Comparison of Optimization Results of CP lines Power System Network Variables

Control variables	ALO	GOT	WOT	SMO
Vg1	1.048846	1.025487	1.001538	1.011778
Vg2	1.045784	1.019055	1.031458	1.001835
Vg3	1.058724	1.007254	1.030804	0.995644
Vg6	1.05166	1.002391	1.056243	1.013476
Vg8	1.053097	1.01082	1.03464	0.982227
Vg9	1.056191	0.988456	1.036079	0.987125
Vg12	1.048186	1.017961	1.043511	0.979016
T18	1.082302	0.997539	1.056928	1.049561
T18	1.084811	1.006531	1.053061	1.020398
T20	1.067459	1.030198	1.063198	1.03373
T25	1.063731	1.040161	1.059091	1.062658
T25	1.059986	0.995673	1.083345	1.049731
T26	1.096323	0.998237	1.093363	0.969746
T29	1.099948	1.033438	1.051269	1.02735
T32	1.071723	1.031114	1.068575	0.956561
T41	1.091173	1.012734	1.071046	0.931446
T45	1.089893	1.022878	1.050636	0.992125
T46	1.06691	0.998583	1.080989	1.037273
T51	1.09508	0.986849	1.057575	0.974174
T49	1.068668	0.957523	1.091433	0.989147
T43	1.079754	1.004732	1.074041	1.041088
T56	1.077691	1.017971	1.07971	1.044692
T57	1.079359	1.036349	1.05546	1.014692
T55	1.067689	0.978286	1.063961	0.878946
Q18	8.30272	10	9.201862	-9.54763
Q25	4.392242	4.82635	3.889286	-6.11097
Q53	0	0	0	-4.58363
Power loss. (p.u)	1.339503	1.338829	1.339377	8.512228
Voltage deviation (VD). (p.u)	0.459004	0.01558	0.096175	0.185308
Stability index (L).	0.027001	0.018269	0.016911	0.338319
Function runs time (seconds).	2.28542	17.9625	0.487161	6.0656

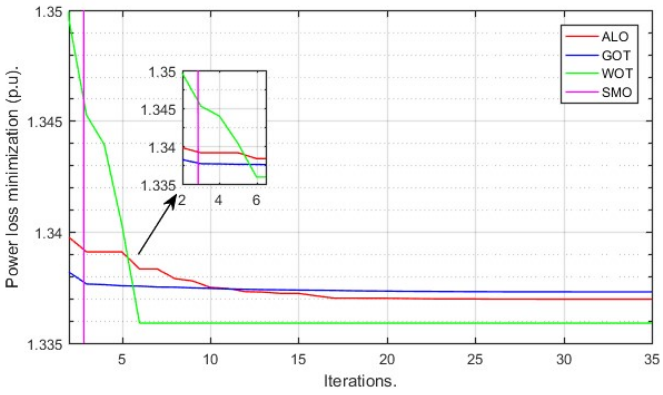

Fig. 16. Power loss minimizations in 3-phase CP lines power system network

0.027. Compared with case 1 and case 2 results the generator voltages (V_g) were considerably increased, the maximum voltage was 1.058 p.u at bus 3 and minimum voltage was 1.0457 p.u at bus 2. Also, the tap settings of transformers increased considerably in this network, the maximum tap setting was 1.0999 at bus 29 and minimum tap setting was 1.0599 at bus 25. Also, the Q_{18} was increased to 8.9027 at bus 18 p.u, Q_{25} was decreased to 4.39 p.u at bus 25 and Q_{53} was decreased to 0 at bus 53.

D) Convergence characteristics.

The convergence characteristics of objective functions of proposed transmission line systems are shown from Fig. 14 to Fig. 16. To explore the variation of convergence characteristics of ALO, GOT, WOT and SMO, the curves were plotted for 15 iterations only. The Fig. 14 is showing the convergence characteristics of the case 1 power system model. The ALO was converged in 25 iterations, the GOT was converged in 35 iterations, WOT was converged in 5 iterations and SMO was converged in 2 iterations.

The Fig. 15 shows the 3-phase PI transmission lines power system convergence. The optimization of system was shown decreasing of number of iterations, the ALO was converged in 16 iterations, GOT was converged in 28 iterations, WOT was converged in 4 iterations and SMO was converged in 5 iterations.

The Fig. 16 shows the convergence characteristics of CP lines power system. It was shown that the ALO was converged in 23 iterations, GOT was converged in 25 iterations, WOT was converged in 6 iterations and SMO was converged in 6 iterations.

In all simulations both ALO and GOT had shown fast convergence characteristics with small deviation of objective functions. Whereas WOT and SMO were converged in less number of iterations, but the convergence speed was very slow. Moreover these algorithms had less exploration of search space.

6. CONCLUSIONS

In this paper the three phase IEEE 57 bus power system network is modeled by using lumped PI lines and distributed CP lines. The performances of the proposed systems were analyzed by using the results of load flow analysis, line parameters frequency response analysis and stochastic optimization algorithms. In literature several published papers were analyzed the frequency dependent transmission lines based power systems. In this paper this effect was neglected in proposed transmission lines based power systems. In this paper the accuracy of CP line was improved by considering the continuous transposition of the line. The load flow simulation results had shown that the percentage error in CP lines system was almost constant irrespective of line length, but in the PI lines system the error was proportional to line length. The simulation of balanced power system models had shown that the error in CP lines system was not more than 13.12%, in PI lines system it was not more than 8% and in positive sequence system it was 8.2%. The simulation of unbalanced power system models had shown that the error in CP lines system was not more than 13.49% and in in PI lines system it was not more than 8.06%. However, the percentage error in short transmission lines has shown random variation in balanced system, but it was smooth in unbalanced system. The frequency response analysis of proposed systems had shown that the PI lines power system is accurate only for low frequency power system operational analysis, such as load flow study and steady state operations. Whereas the CP lines power model the line parameters were constant for low frequency power system operational analysis, but for high frequency operations such as transients the magnitude of line parameters were increasing proportionally. The simulation results were described that the PI lines system behaves as low pass filter which attenuates the high frequency waves and the CP lines system behaves as high pass filter which attenuates the low frequency waves.

Also, the capability of proposed power system models were tested by using ALO, WOT, GOT and SMO optimization algorithms to minimize the total power loss (P_{loss}) with addition of penalty factors, such as minimum voltage deviation (VD), and minimum voltage stability index (L). The optimization results were described the best setting of generator voltages (V_g), tap setting of transformers (T) and shunt capacitors (Q_c). When compared the results of ALO with other algorithms, it was shown that the ALO had best exploration capability of variables, and excellent convergence characteristics. Due to this high exploration capability of ALO, it had described the best positions of all control variables for all proposed models. But due to low elitism and less exploration capability of other proposed algorithms, it was noticed that the setting of variables results trivial. The execution time of ALO was very less due to high convergence characteristics. It was observed that the results of GOT and ALO were similar

with small deviation. The results of WOT and SMO had shown slow convergence of objective function, it was due to the less exploration capability of these algorithms. It had been observed that the ALO shown small variation of convergence curves for optimization of all proposed models. When compared the results of Table 5 with all optimization results, the CP lines system has given accurate results.

REFERENCES

[1] H. W. Dommel, "Digital computer solution of electromagnetic transients in single and multiphase networks", *IEEE Trans. Power Apparatus Syst.*, vol.88, no. 4 pp. 388– 399, 1969.

[2] J. R. Marti, "Accurate Modeling of Frequency-Dependent Transmission Lines in Electromagnetic Transient Simulations," *IEEE Trans. Power Apparatus Syst.*, vol. 101, pp. 147–157, 1982.

[3] Bjorn Gustavsen, Garth Irwin,Ragnar Mangelrod, Dennis Braandt and Kelvin Kent, "Transmission Line Models for The Simulation of Interaction Phenomena Between Paralel AC and DC Oerhead Lines," *Int. Conf. Power Syst. Transie.*, Budapest-Hungary, pp. 20–24, 1999.

[4] MEHMET SALIH MAMIS¸ and MUHAMMET KOKSAL, "Remark on the Lumped Parameter Modelling of Transmission Lines," *IEEE Trans. Power Syst.*, vol. 28, no. 6, pp 565–575, 2000.

[5] YUAN LIAO, "Equivalent PI Circuit for Zero-sequence Networks of Parallel Transmission Lines," *Electric Power Compon. Syst.*, vol. 37, no. 7, pp 787–797, 2009.

[6] D. E. Hedman,"Propagation on Overhead Transmission LinesI-Theory of Modal Analysis," *IEEE Winter Power Meeting*, New York, N. Y., vol. 65, no. 101, pp 200–205, 1965.

[7] Clayton R. Paul, "Decoupling the Multi conductor Transmission Line Equations," *IEEE Trans. Microwave Theory Tech.*, vol. 44, no. 8, pp 1429–1440, 1996.

[8] F Castellanos, J R Marti, and F Marcano, "Phase-domain multiphase transmission line models," *Elec. Power Energy Syst.*, vol. 19, no. 4, pp 241–248, 1997.

[9] H.V. Nguyen, H.W. Dommel, and J.R. Marti, "Direct Phase-Domain Modelling of Frequency-Dependent Overhead Transmission Lines," *IEEE Trans. Power Delivery*, vol. 12, no. 3, pp 1335–1342, 1997.

[10] Atef Morched, Bjorn Gustavsen, and Manoocher Tartibi, "A Universal Model for Accurate Calculation of Electromagnetic Transients on Overhead Lines and Underground Cables," *IEEE Trans. Power Delivery*, vol. 14, no. 3, pp 1032–1038, Jul. 1999.

[11] M. C. Tavares, J. Pissolato, and C. M. Portela," Mode Domain Multiphase Transmission Line Model - Use in Transient Studies" *IEEE Trans. Power Delivery*, vol. 14, no. 4, pp 1533–1544, Oct. 1999.

[12] S. Kurokawa, , E.C. Costa, , J. Pissolato, , A.J. Prado, and L.F. Bovolato, "Proposal of a Transmission Line Model Based on Lumped Elements: An Analytic Solution," *Elec. Power Compon. Syst.*, vol. 38, no. 14, pp 1577–1594, Dec. 2010.

[13] N.V. Souza, , C.G. Carvalho, , S. Kurokawa, and J. Pissolato, , "A Distributed-parameters Transmission Line Model Developed Directly in the Phase Domain," *Elec. Power Compon. Syst.*, vol. 41, no. 11, pp 1100–1113, 2013.

[14] C.G.D. Carvalho, , E.C.M. Costa, , S. Kurokawa, and J. Pissolato, , "Alternative Phase-domain Model for Multi Conductor Transmission Lines Using Two Modal Transformation Matrices," *Elec. Power Compon. Syst.*,, vol. 44, no. 3, pp 291–301, Dec. 2015.

[15] S. Kurokawa, , M.C. Tavares, , C.M. Portela, and A.J. Prado, , " Behavior of Overhead Transmission Line Parameters on the Presence of Ground Wires," *IEEE Trans. Power Delivery*, vol. 20, no. 2, pp 1669–1676, 2005.

[16] A. De Conti, and M.P.S. Emídio, ," Extension of a modal-domain transmission line model to include frequency-dependent ground parameters," *Elec. Power Syst. Research*, vol. 138, no. 17, pp 120–130, 2016.

[17] P. T. Caballero, E. C. Marques Costa, and S. Kurokawa," Fitting the frequency-dependent parameters in the Bergeron line model," *Elec. Power Syst. Research*, vol. 117, no. 2 pp 14 – 20, 2014.

[18] P. T. Caballeroa, E. C. M. Costab, S. Kurokawa, "Frequency-dependent multi conductor line model based on the Bergeron method," *Elec. Power Syst. Research*, vol. 127, no. 33, pp 314–322, 2015.

[19] A. R. J. Araujo, R. C. Silva, and S. Kurokawa, "Representation of Transmission Lines: A Comparison between the Models Distributed Parameters and Lumped Parameters" *IEEE Lat. Am. Trans.*, vol. 11, no. 4, pp 1047–1052, 2013.

[20] A. Ramirez, J. L. Naredo, and P. Moreno, "Full Frequency-Dependent Line Model for Electromagnetic Transient Simulation Including Lumped and Distributed Sources," *IEEE Trans. Power Delivery*, vol. 20, no. 1, pp 292–299, 2005.

[21] H. Ye, and K. Strunz," Multi-Scale and Frequency-Dependent Modeling of Electric Power Transmission Lines," *IEEE Trans. Power Delivery*, vol. 33, no. 1, pp 32–41, 2018.

[22] J. A. Rosendo Macias, A. G. Exposito, and A. B. Soler," A Comparison of Techniques for State-Space Transient Analysis of Transmission Lines," *IEEE Trans. Power Delivery*, vol. 20, no. 2, pp 894–903, 2005.

[23] H. Ye, and K. Strunz," Modal decoupling of overhead transmission lines using real and constant matrices: Influence of the line length," *Elec. Power Energy Syst.*, vol. 92, no. 18, pp 202–2011, 2017.

[24] U. Leeton, D. Uthitsunthorn, U. Kwannetr, N. Sinsuphun and T. Kulworawanichpong, "Power loss minimization using optimal power flow based on particle swarm optimization," *ECTI-CON2010: The 2010 ECTI Int. Conf. Elec. Eng./Electron. Computer, Telecommun. Info. Techno.*, Chiang Mai, 2010, pp. 440–444.

[25] S. Mouassa, , T. Bouktir, and A. Salhi. "Ant lion optimizer for solving optimal reactive power dispatch problem in power systems." *Eng. Sci. Techno. Int. J.* 20, no. 3, 885–895, 2017.

[26] A. Rajan, , K. Jeevan, and T. Malakar. "Weighted elitism based Ant Lion Optimizer to solve optimum VAr planning problem." *Appl. Soft Comput.*, vol. 55, 352-370, 2017.

[27] Mirjalili, Seyedali. "The ant lion optimizer." *Adv. Eng. Software*, 83, 80-98, 2015.

[28] Saremi, Shahrzad, Seyedali Mirjalili, and Andrew Lewis. "Grasshopper optimisation algorithm: theory and application." *Adv. Eng. Software*, vol. 105, 30–47, 2017.

[29] Mirjalili, Seyedali, and Andrew Lewis. "The whale optimization algorithm." *Adv. Eng. Software*, 95, 51-67, 2016.

[30] Bansal, Jagdish Chand, Harish Sharma, Shimpi Singh Jadon, and Maurice Clerc. "Spider monkey optimization algorithm for numerical optimization." *Memetic computing*, vol. 6, no. 1, 31–47, 2014.

[31] College of Engineering, Electrical Engineering, University of Washington, *Power System Test Case Archive*, Nov. 2013. [Online]. Available: http://www.ee.washington.edu/research/pstca/

[32] Ramasamy Natarajan, "Computer-Aided Power System Analysis," 1st ed., *New York, Basel, USA: Marcel Dekker, Inc.*, 2002, Table 2.1.